Optimal sizing and design of renewable power plants in rural microgrids using multi-objective particle swarm optimization and branch and bound methods

Carlos Roldán-Blay [*], Guillermo Escrivá-Escrivá, Carlos Roldán-Porta, Daniel Dasí-Crespo

Institute for Energy Engineering, Universitat Politècnica de València, Camino de Vera, s/n, edificio 8E, escalera F, 2ª planta, 46022, Valencia, Spain

ABSTRACT

As energy prices rise, optimizing renewable power plant sizing is vital, especially in areas with unreliable electricity supply due to distant transmission lines. This study addresses this issue by optimizing a renewable power plant portfolio for a Spanish municipality facing such challenges. The presented approach involves a systematic method. Firstly, energy demand is thoroughly analyzed. Next, available renewable resources are explored and optimal plant placements are determined. A multi-objective particle swarm optimization algorithm is then used to size each plant, minimizing annualized costs and grid energy imports. The most suitable feasible optimum is selected from theoretical configurations using branch and bound techniques, prioritizing practicality. In the specific case analyzed, the results show a 20-year Internal Rate of Return of 8.33 %. This is achieved with the following capacities for each plant: 750 kW of photovoltaic solar energy, 160 kW of turbine-based generation, 180 kW of hydroelectric pumping, 160 kW for the biomass plant, and 200 kW from the wind turbine. This study offers an innovative solution to energy challenges, providing practical insights for cost-efficient, sustainable projects.

1. Introduction

Electricity prices have been steadily increasing due to various factors. The primary driver of this increase has been the growing demand for electrical energy, exacerbated by the limited capacity of the system [1]. Additionally, the depletion of fossil resources has contributed to a rise in energy prices, a trend that has intensified since the second half of 2021 [2]. To effectively address these challenges, it is imperative to adopt a multifaceted approach, both on the demand and electricity generation sides.

On the demand side, cost reduction and mitigation of energy prices can be achieved by aligning consumption with system conditions, both at small [3] and large scales [4]. As a result, substantial efforts have been invested in research to improve demand response mechanisms [5] and encourage active consumer participation in the electricity market operations [6].

On the generation side, attention is also required. Increased utilization of renewable energy sources has reduced dependence on fossil fuels [7], leading to a decrease in energy costs [8]. In this context, microgrids (MGs) have emerged as a viable solution to integrate these renewable

sources [9]. MGs facilitate distributed and centralized utilization of renewable energy facilities [10]] as they are allowed to operate independently [11]. This enables small-scale distributed generation facilities to enhance system reliability [12] and reduce dependence on traditional centralized facilities [13]. Typically, these MGs remain interconnected with the main grid [14], optimizing overall system performance through the management of their micro power plants [15]. However, they can operate autonomously, further enhancing reliability in case of supply interruptions [16]. For this purpose, an energy storage system is required in most cases [17]. Nevertheless, to fully realize the advantages offered by MGs to the electrical system and its participants [18], efficient design is essential, requiring the establishment of reliable and appropriate methodologies [19].

The first step in designing an MGs power supply system involves analyzing consumer demand patterns. Subsequently, an examination of available natural resources is necessary to propose an optimal mix of generation (and storage). Finally, the design of components, including their locations and sizes, must be optimized [20]. While determining locations is often straightforward due to physical constraints, sizing elements can be more complex. In general, the objective is to select a combination of resources that minimizes installation costs, taking into

Nomenclature

BAB	Branch and bound
MG	Microgrid
PSO	Particle swarm optimization
PV	Photovoltaic

Parameters, variables, and functions

C_{E_y}	Yearly costs of energy supplied by the grid (€/year)
C_{I_i}	Installation costs of resource i (€)
C_{I_y}	Yearly installation costs (investments) of the generation facilities (€/year)
C_{M_y}	Yearly maintenance costs of the generation facilities (€/year)
C_{M_i}	Yearly maintenance costs of resource i (€/year)
C_{O_i}	Yearly operating costs of resource i (€/year)
C_{O_y}	Yearly operating costs of the generation facilities (€/year)
C_y	Yearly costs of generation facilities (€/year)
c_i	Function to represent the installation costs of resource i given its installed power (€)
c_1	Acceleration coefficient to update a particle's velocity (self adjustment weight)
c_2	Acceleration coefficient to update a particle's velocity (social adjustment weight)
$E_{H_{max}}$	Maximum energy that can be stored in the hydroelectric power plant (kWh)
$E_{H_{min}}$	Minimum energy that can be stored in the hydroelectric power plant (kWh)
E_{H_o}	Initial energy stored in the hydroelectric power plant (kWh)
f	Objective function
f_n	Normalised value of the objective function
f_1	First objective function (yearly costs of generation facilities)
f_2	Second objective function (energy supplied by the grid)
$f_{1_{max}}$	Maximum value of the first objective function used to normalise them
$f_{2_{max}}$	Maximum value of the second objective function used to normalise them
f_{1_n}	Normalised value of the first objective function
f_{2_n}	Normalised value of the second objective function
$g^{(s)}$	Global best position in the swarm as of iteration s
m_{f_i}	Fixed maintenance costs of resource i (€)
m_{v_i}	Variable maintenance costs of resource i (€/h)
n_y	Project lifetime (years)
o_{f_i}	Fixed operating costs of resource i (€)
o_{v_i}	Variable operating costs of resource i (€/h)

P_i	Installed power of resource i (decision variables) (kW)
PF_i	Set of feasible values of decision variable i (decision variable feasible range) (kW)
$P_{i_{max}}$	Maximum value of installed power of resource i (decision variable bounds) (kW)
$P_{i_{min}}$	Minimum value of installed power of resource i (decision variable bounds) (kW)
$p_d(t)$	Demanded power at time t (W)
$p_g(t)$	Power supplied by the grid at time t (W)
$p'_H(t)$	Power extracted from the storage system in the hydroelectric power plant at time t (W)
$p_P(t)$	Power demanded by pumps at time t (W) (kW)
$\hat{p}_{BM}(t_p)$	Average power supplied by the biomass power plant during the time interval t_p (kW)
$\hat{p}_d(t_p)$	Average demanded power during the time interval t_p (kW)
$\hat{p}_H(t_p)$	Average power supplied by the hydroelectric power plant during the time interval t_p (kW)
$\hat{p}_g(t_p)$	Average power supplied by the grid during the time interval t_p (kW)
$\hat{p}_i(t_p)$	Average power supplied by resource i during the time interval t_p (kW)
RS	Set of resources considered in the project. In this study, the resources considered are PV (photovoltaic), P (hydraulic pumps), T (hydraulic turbines), BM (biomass) and W (wind) generators
r	Interest rate (%)
r_1, r_2	Random values to randomise a new particle's velocity calculation
t_i	Total time of use of resource i during the project lifetime (h)
$v_k^{(s)}$	Velocity of particle k at iteration s
$x_k^{(s)}$	Position of particle k at iteration s
$\hat{x}_k^{(s)}$	Best position of particle k as of iteration s
α	Inertial coefficient to update a particle's velocity
γ	Annual demand growth (%)
ε_j	Weight of the first objective function for each optimization problem to search a Pareto front solution (non-dominated solution)
η_P	Efficiency of hydraulic pumps (%)
η_T	Efficiency of hydraulic turbines (%)
$\mu_i(n)$	Binary function that equals 1 if resource i has maintenance costs at year n
$\omega_i(n)$	Binary function that equals 1 if resource i has operating costs at year n

account economic investments [21]. However, specific constraints may vary from one case to another [22]. Furthermore, optimizing the design of an MG involves considering multiple objectives [23]. For instance, consumers in certain geographical areas may experience reliability issues due to challenging terrain and adverse weather conditions, such as wind and snow, resulting in long distribution lines [24]. In such cases, installing various renewable energy plants to meet electricity demand can significantly improve the situation [25]. Consequently, reducing dependence on the general electrical grid becomes a key goal in designing these MGs [26]. These projects involve substantial investments that need to be minimized [27] and must comply with all physical and legal constraints associated with various facilities [28].

Therefore, addressing such issues requires the use of multi-objective optimización techniques with constraints [29]. To tackle such cases, numerous multi-criteria optimization techniques have been used in the literature [30]. These techniques have been primarily employed to enhance system resilience [31], reliability [32] and stability [33]. In addition, other studies have utilized these techniques to establish new solutions in economic dispatch [34]. Furthermore, they have also been applied to optimize network management [35]. On the other hand, plant size optimization during the planning phase with multi-criteria optimization techniques has been analyzed. In the latter case, there are studies aiming to minimize both installation costs at the initial investment level [36] and operation costs over its lifetime [37]. However, there is a gap in the current literature regarding the joint consideration of planning and management phases, particularly in rural areas [38]. Additionally, most existing studies do not emphasize the importance of energy supply reliability enough, especially in rural areas. While some studies have addressed reliability [39], it has not been a focal point in the optimization process [40]. Furthermore, the utilization of available
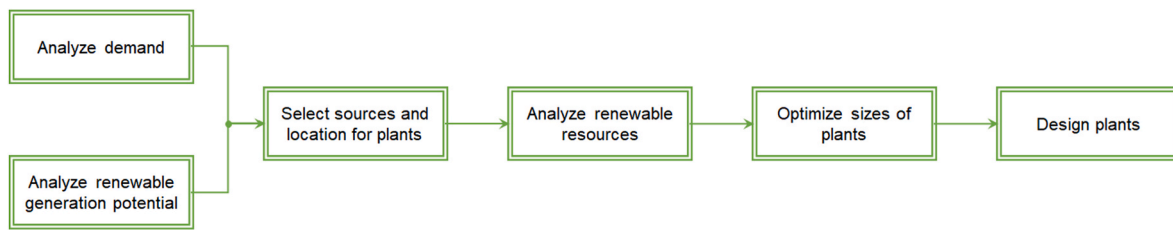
Fig. 1. Flowchart for optimal design of the generation infrastructure of a microgrid.

natural resources (such as waste biogas or river water energy) and specific geographical advantages of case studies are not adequately explored. The focus has primarily been on meeting the needs of the environment [41] rather than harnessing its strengths.

Therefore, this paper presents the optimal design of generation infrastructure for a real MG in a rural area of Spain using a method based on multi-objective particle swarm optimization (PSO) [42] combined with the search for a feasible optimum using the branch and bound (BAB) technique [43]. Two objective functions have been selected to address the unique needs of rural areas, focusing on improving reliability and minimizing the costs of the designed facilities. The PSO algorithm has been chosen for its simplicity [44] and computational efficiency [45], as it produces high-quality solutions quickly and exhibits stable convergence [46]. Moreover, it has a proven track record in solving electricity systems optimization, as shown in Ref. [47], even with multiple scenarios [48]. Finally, the incorporation of legal constraints on plant sizes and the use of discrete variables instead of continuous ones further increase the complexity of the problem, highlighting a clear research gap in the existing literature.

The methodology developed in this work provides a comprehensive overview of its general application in optimizing the design of MG generation plants while addressing the minimization of annualized installation costs and imported energy from the grid. The methodology generates a set of Pareto frontier points, representing scenarios that minimize both objective functions while considering their interrelation. The methodology is exemplified through a case study involving the design of an actual MG in a Spanish municipality. The application of the methodology is described, the selection of the optimal solution is discussed, and a detailed description of the final designed facilities is provided, including the technical feasibility analysis of the MG. It is noteworthy that this case study represents a significant innovation, as it considers the minimization of energy imported from the grid and allows for the development of an MG with substantial improvements in the reliability of electric energy supply. The inclusion of this objective enables the assessment of the MGs potential to operate in an isolated mode or be designed for such operation [49]. This case study is also pioneering in Spain, potentially making the municipality the first in the country to disconnect from the general electricity grid. By employing the proposed method, optimal solutions are obtained that minimize or even eliminate exchanges with the grid, offering a range of scenarios that are highly valuable for installations with low power quality due to a weak connection to the system.

The main contributions of this work are listed below:

- The described method provides a set of viable optimal solutions applicable to both continuous and discrete variables. To determine the optimal solution, BAB is applied to the best solutions from the Pareto frontier, ensuring optimality and convergence speed during the PSO algorithm.
- The proposed method enables the optimal design of MG generating facilities, aiming to minimize costs and exchanges with the grid. This approach facilitates the feasibility assessment of creating an MG capable of operating in isolation (islanded operation). By doing so, it enhances the MG's reliability, decoupling it from grid failures.

Moreover, the method considers not only the initial investment but also the total annualized cost.
- The presented case study is the first of its kind in Spain, involving the development of a real project for MG infrastructure. The case study is presently undergoing construction, during which a detailed description of the optimization methodology, data analysis, and the final design of the microgrid is provided.

The article follows the subsequent structure. Section 2 furnishes an extensive account of the proposed methodology. Section 3 employs the methodology in a real case study, scrutinizes the outcomes, and deliberates on the choice of the optimal solution. In Section 4, the chosen optimal solution's technical implementation is delineated, encompassing considerations of both physical and legal impediments. A comprehensive examination of various installations and a technical feasibility analysis of the microgrid complex are expounded upon. Lastly, Section 5 presents conclusions derived from the work presented.

2. Materials and methods

This section describes the proposed method for the optimal design of the generation infrastructure of a MG. In general, the method corresponds to the one shown in Fig. 1, in order to be applied to any location. As this section will show, the proposal involves a systematic and integrated method for sizing renewable power plants. This includes demand analysis, resource assessment, optimal placement, and the application of a multi-objective particle swarm optimization algorithm, combined with a discussed selection of the optimal feasible solution to be implemented.

Therefore, the first thing is to analyse the electrical demand needs to be covered with the installations to be designed [50]. For this, records of hourly electricity consumption of at least one year are required. In addition, it is convenient to know maximum instantaneous power values to take them into account in the final detailed design. The probability distribution of the hourly energy demand must be obtained. Likewise, the generation potential of the different available resources must be studied in order to evaluate their feasibility and estimate their performance and probability distribution.

The next step would be to select the available sources that can meet the hourly demand. For this, the previous analysis is used, discarding the sources that are not profitable. Examples of typical resources can be photovoltaic (PV) solar power plants, wind power plants, storage systems such as batteries or hydroelectric plants or biomass or biogas plants. For the selected sources, the optimal location must be decided, considering the availability of resources and their performance.

Next, the actual resource available from the selected sources must be studied. At a minimum, an estimate of the specific generation of each source (typical generation per installed kW) must be calculated. Additionally, the limits of the facilities that require storage or use of raw material must be calculated (maximum size of the deposits for hydroelectric plants or the amount of biomass that can be collected and stored per day).

After having these basic data, a multi-criteria optimization algorithm must be implemented to design the optimal sizes of each power plant (in kW), minimizing the total annualized cost and the energy imported from the general network. To this end, the use of an algorithm based on multi-

objective particle swarm optimization is proposed together with a final search for the feasible optimum by BAB. In addition, once the Pareto frontier is obtained, the selection of the optimal scenario must be discussed considering all the legal and physical restrictions. In this analysis, criteria such as minimization of costs, environmental impact or balanced use of available natural resources must be considered, among others.

The multi-criteria optimization method used in this study is described below. First, the mathematical approach to the optimization problem is shown. To do this, both the decision variables and the objective functions are defined. Then the algorithms to obtain set of optimal solutions of the Pareto frontier are explained. The results of the optimization in the developed case study are shown in later sections.

2.1. Objective functions

The main objective function to be minimized is the total annualized cost of electricity supply to meet demand. Equation [1] corresponds to the first objective function:

$$f_1 = C_y \qquad (1)$$

On the other hand, it is desired to minimize the exchange of energy with the network due to the low reliability that has historically been seen with the traditional configuration. This is done with the intention of approaching a hypothetical future situation of system disconnection. Thus, the second objective function is the one shown in equation [2]:

$$f_2 = \int_0^{8760} p_g(t)dt \qquad (2)$$

where $p_g(t)$ is the power imported from the network at each moment of the study year. Therefore, the general statement of the objective of this problem would correspond to equation [3]:

$$min\, f = min\,(f_1, f_2) \qquad (3)$$

The annualized cost has four components, as shown in equation [4]:

$$C_y = C_{I_y} + C_{O_y} + C_{M_y} + C_{E_y} \qquad (4)$$

where C_{I_y} is the cost of the investments required to install the infrastructure of the electricity supply systems, C_{O_y} and C_{M_y} are the annualized operation and maintenance costs of the set of systems for electricity supply, respectively and C_{E_y} is the total cost of energy imported from the grid.

For each disbursement occurring in different years, and under the assumption of a given interest rate r it is possible to calculate the annualized costs associated with these disbursements throughout the study's n_y year horizon, using the equations [5–7]:

$$C_{I_y} = \frac{\sum C_{I_i}}{n_y}, \forall i \in RS \qquad (5)$$

$$C_{O_y} = \frac{\sum_{j=0}^{n_y-1} \frac{C_{O_i}}{\left(1+\frac{r}{100}\right)^j}}{n_y}, \forall i \in RS \qquad (6)$$

$$C_{M_y} = \frac{\sum_{j=0}^{n_y-1} \frac{C_{M_i}}{\left(1+\frac{r}{100}\right)^j}}{n_y}, \forall i \in RS \qquad (7)$$

In these expressions, RS is the set of resources, for example, PV, hydropower (pumps and turbines), biomass and wind.

2.1.1. Cost determination

To calculate the investment costs, it is necessary to know the sizes of each installation. Depending on them, the cost C_I of each resource will be obtained as shown in equation [8]:

$$C_{I_i} = c_i(P_i), \forall i \in RS \qquad (8)$$

The sizes of the facilities P_i are the variables to be determined to minimize the objective function, called decision variables. Once these sizes have been set, the operation and maintenance costs are obtained by carrying out the load flow of each situation for a full year and analyzing the use of the facilities. Estimating a certain cost for each amount of kWh generated from each resource and updating the demand for each year with an estimated percentage increase of γ and the same probability distribution as the one studied, the operation and maintenance cost of each resource can be obtained in every year n using equations [9,10]:

$$C_{O_i}(n) = o_{v_i} \cdot t_i \left(p_d(t) \cdot \left(1 + \frac{\gamma}{100}\right)^n, P_1, ..., P_k \right) + o_{f_i} \cdot \omega_i(n), \forall i \in RS \qquad (9)$$

$$C_{M_i}(n) = m_{v_i} \cdot t_i \left(p_d(t) \cdot \left(1 + \frac{\gamma}{100}\right)^n, P_1, ..., P_k \right) + m_{f_i} \cdot \mu_i(n), \forall i \in RS \qquad (10)$$

where o_{v_i} and o_{f_i} are the annual variable and fixed operation costs of resource i, respectively. t_i is the time of use of that resource for year n, which depends on the demand for that year (updated with the assumed increase γ). m_{v_i} and m_{f_i} are the annual variable and fixed costs, respectively, of maintenance of resource i and the fixed costs of operation and maintenance take place, respectively, in those years in which the functions $\omega_i(n)$ and $\mu_i(n)$ are not zero.

As can be seen, the time each resource is used depends on the sizes of all the resources, as indicated by the equations. Therefore, in each iteration it will be necessary to use an algorithm (such as DEROP [51] to obtain the use of each resource at each moment during the simulation period. Thus, this objective function is a noisy function, that is, it has no explicit expression.

2.1.2. Energy provided by the network determination

Similarly, to obtain the value of the second objective function for an interval of one year, for example, it is necessary to complete the optimal load flow for the entire evaluation period. In this way, the energy provided by the grid can be obtained using equation [11], instead of using equation [2].

$$f_2 = \int_0^{8760} \left(p_d(t) + p_P(t) - \sum_i p_i(t) \right) dt, \forall i \in RS \backslash \{P\} \qquad (11)$$

where $p_d(t)$ is the power demanded at each moment of the year, $p_P(t)$ is the power demanded by the pumps of the hydroelectric plant and $p_i(t)$ is the power provided by each one of the resources of the contemplated set (of which pumps have been excluded, as they are considered an additional load).

When computing the value of this function for a certain value of the decision variables P_i, an algorithm is proposed whose rules are set out below.

a) For each iteration, the demand curve is generated following the studied distributions and considering the proposed annual growth γ.
b) The generation curve of resources such as PV and wind power are also generated using the value of their variables P_i and the corresponding distributions. The generation is limited to a value such that exports do not take place, so that for each time interval t_p its value must comply with the restriction [12].

$$\sum_{i \in \{PV, W\}} \widehat{p}_i(t_p) \le \widehat{p}_d(t_p) \qquad (12)$$

c) Resources such as biomass are used as base production. The production curve of a resource such as biomass is the maximum value

that it can generate without exporting energy to the grid, for all hours of each day except the hours of greatest renewable production. In other words, the generation of a biomass power plant during these hours depends on the demand and the generation of systems such as PV or wind power and corresponds to equation [13]:

$$\widehat{p}_{BM}(t_p) = \begin{cases} min\left(p_d(t_p) - \sum_{i \in \{PV,W\}} p_i(t_p), P_{BM}\right), & p_d(t_p) > \sum_{i \in \{PV,W\}} p_i(t_p) \\ 0, & p_d(t_p) = \sum_{i \in \{PV,W\}} p_i(t_p) \end{cases}$$

(13)

d) The power curve provided by a storage system, such as a hydro-electric plant, is such that as much as possible is pumped or turbined each hour. Therefore, equation [14] is used, taking the power supplied by this system as a positive value:

$$\widehat{p}_H(t_p) = \begin{cases} min\left(\widehat{p}_d(t_p) - \sum_{i \in \{PV,W,BM\}} \widehat{p}_i(t_p), \frac{\eta_T}{100} \cdot P_T\right), & p_d(t_p) \geq \sum_{i \in \{PV,W,BM\}} p_i(t_p) \\ -min\left(\sum_{i \in \{PV,W,BM\}} \widehat{p}_i(t_p) - \widehat{p}_d(t_p), \frac{\eta_P}{100} \cdot P_P\right), & p_d(t_p) < \sum_{i \in \{PV,W,BM\}} p_i(t_p) \end{cases}$$

(14)

where P_T and P_P are the decision variables corresponding to the installed power of turbines and pumps, respectively and η_T and η_P their respective performances.

e) In storage resources, it is necessary to control that the total energy stored during the entire simulation period is within the appropriate limits. To simplify the problem, the maximum capacity and depth of discharge of these systems can be fixed. Otherwise, it will be necessary to choose an additional decision variable for these systems. The condition that must be met is shown in equation [15].

$$E_{H_{min}} \leq -\int_{-\infty}^{t_p} p'_H(t) \cdot dt = E_{H_o} - \int_{t_0}^{t_p} p'_H(t) \cdot dt \leq E_{H_{max}}$$

(15)

In equation [15], $p'_H(t)$ is the energy leaving the storage system, where each energy flux in equation [14] is divided by its corresponding output, $E_{H_{min}}$ and $E_{H_{max}}$ are the minimum and maximum limits, respectively, of the energy stored in the system and E_{H_o} is the energy stored at the initial instant of the simulation.

f) Finally, the import from the network at each moment will be the power that is not supplied by any generation system. Therefore, this value will be obtained using equation [16]:

$$\widehat{p}_g(t_p) = min\left(p_d(t_p) - \sum_{i \in \{PV,W,BM,H\}} p_i(t_p), 0\right)$$

(16)

2.2. Multi-objective optimization problem

In order to address the optimization problem, the process commences by standardizing the objective function using the equation [17]:

$$f_n = (f_{1_n}, f_{2_n}) = \left(\frac{f_1}{f_{1_{max}}}, \frac{f_2}{f_{2_{max}}}\right)$$

(17)

Once normalised, the problem consists of minimizing said function subject to the restriction of minimum and maximum values of the decision variables. This is shown in equation [18].

$$\begin{aligned} &minimise & f_n \\ &subject\ to & \begin{cases} P_{i_{min}} \leq P_i \leq P_{i_{max}} \forall i \\ P_i \in PF_i \forall i \end{cases} \end{aligned}$$

(18)

where PF_i is the set of feasible discrete values for variable P_i.

To solve this problem, the proposed optimization method based on a MOPSO and a final BAB technique are used. This procedure is necessary because it deals with constrained noisy functions and because it has discrete decision variables and with lower and upper bounds. The algorithm is explained below.

2.3. Proposed optimization algorithm

To solve the proposed problem, a set of parameters $\varepsilon_j \in [0, 1]$ is defined to pose various single objective optimization problems. Therefore, for each parameter ε_j there is an optimization problem whose solution is a point on the Pareto frontier. The objective function of each of these problems is obtained by means of equation [19]:

$$f_j = \varepsilon_j \cdot \frac{f_1}{f_{1_{max}}} + (1 - \varepsilon_j) \cdot \frac{f_2}{f_{2_{max}}}, 0 \leq \varepsilon_j \leq 1$$

(19)

Each of these optimization problems is solved by minimizing the corresponding objective function f_j with a PSO algorithm considering the following remarks:

a) For each combination of the variables P_i, the use of each system and the total cost of energy must be calculated to obtain the value of the objective function. Since it is not possible to obtain this function explicitly, the value of this function is calculated after simulating the load flow of all the systems during the evaluation period, based on the known demand curve and the forecast growth estimate. That is, the objective functions are noisy functions, which requires the use of multi-objective optimization algorithms such as the proposed MOPSO with a search for the feasible optimum through BAB.

b) The variables P_i are generally discrete, so they have a minimum value, a maximum value, and a finite number of feasible intermediate values. The problem will be solved continuously to prevent rounding from affecting particle speed and convergence. After finishing, a BAB technique will be used to find the best feasible solution close to the theoretical optimum obtained.

c) As a consequence of the above, after the last iteration, if a variable falls between two possible values, the BAB technique will be applied to determine the best feasible solution. That is, if at the end of the iterative process a variable P_i obtains a value of P_h and the closest possible values for it are P_a and P_b with $P_a < P_h < P_b$, the value of the objective function $f_j = f_a$ will be calculated considering $P_i = P_a$ and the value $f_j = f_b$ when $P_i = P_b$ and the value that minimizes the objective function $f_j = min(f_a, f_b)$ will be chosen. If this happens for several variables simultaneously, the value of the objective function will be calculated for all the possible combinations and the combination that minimizes it will be chosen, exploring the tree of combinations and choosing the best ones through BAB. Thus, in a general case with n_r resources, it would be necessary to simulate up to 2^{n_r} possible combinations and choose the one that minimizes the objective function. Note that in some of these cases it may happen that a solution is not viable because it does not satisfy some restriction, so it would be necessary to modify all the variables one step up or down and explore scenarios and discard those that are not optimal. As a result of the process, the optimal viable solution closest to the theoretical optimum is reached.

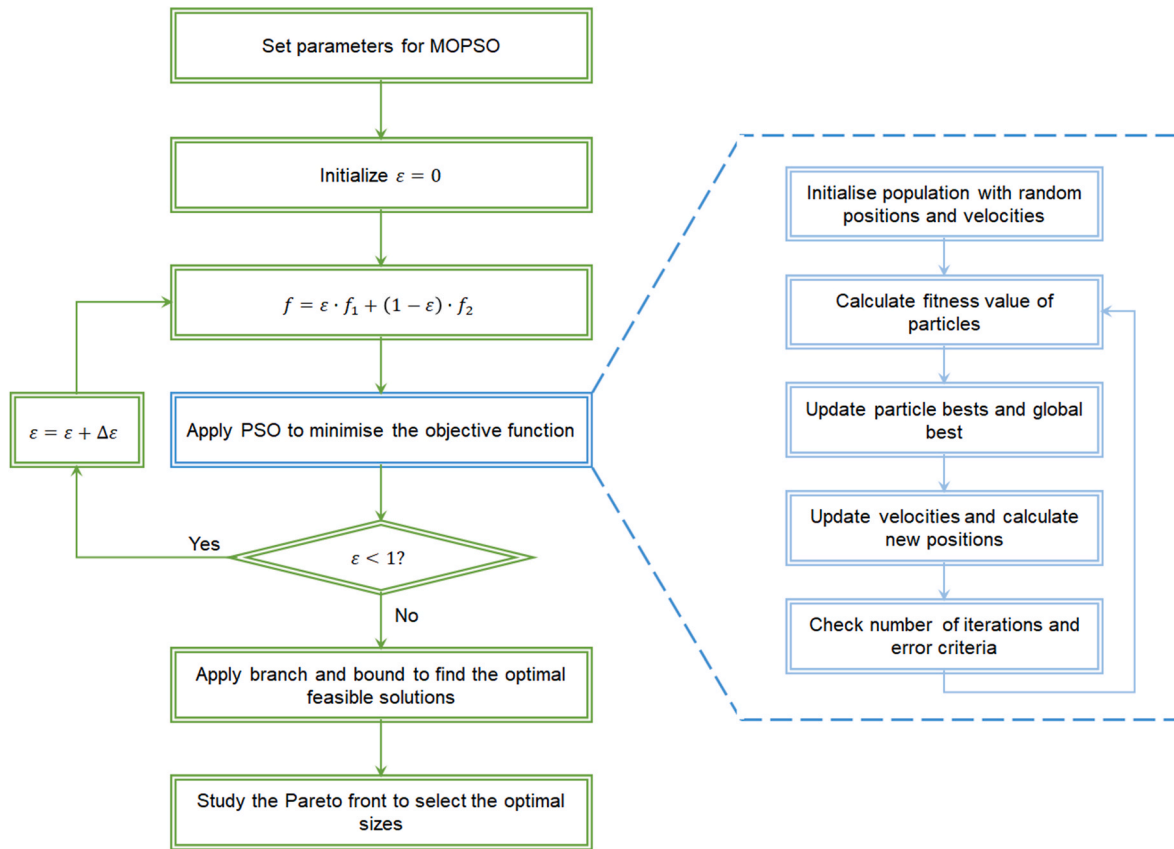The PSO algorithm is used normally in all other respects, as described below.

Fig. 2. Flow chart to optimize plant sizing.

2.3.1. Particle swarm optimization algorithm

The PSO algorithm consists of an iterative process in which some particles take positions that tend to the optimum of the objective function to be minimized. There is an extensive bibliography on this [52], so in this section only the stages of the algorithm are summarized. The movement of the particles simulates the movement of a swarm. The particles are vectors that contain the decision variables of the problem and their positions are the values they take at each moment. To do this, three steps are followed:

1. Evaluate the fitness value of each particle at the current position. That is, compute the value of the objective function at the current position of each particle.
2. Update the best individual fitness of each particle and the best global fitness.
3. Update each particle's velocity and its new position for the next iteration.

The initial positions of the particles are taken uniformly distributed trying to cover the entire space of feasible values of each decision variable. In each iteration, each particle obtains a fitness value (value of the objective function) and remembers its best value throughout the algorithm. In each iteration, the particle with the best fitness value is also updated, comparing it with the best value obtained in the previous iterations. Typical stopping criteria can be the number of iterations or the tolerance [53] (small changes in the best fitness value).

At each iteration s, the position of each particle k in the population is updated using equation [20]:

$$x_k^{(s+1)} = x_k^{(s)} + v_k^{(s+1)} \qquad (20)$$

where x is the position and v is the velocity of the particle. The velocity must be calculated using equation [21]:

$$v_k^{(s+1)} = \alpha \cdot v_k^{(s)} + c_1 \cdot r_1 \cdot \left(\widehat{x}_k^{(s)} - x_k^{(s)} \right) + c_2 \cdot r_2 \cdot \left(g^{(s)} - x_k^{(s)} \right) \qquad (21)$$

where i is the particle index, α is the inertial coefficient, c_1 and c_2 are acceleration coefficients ($0 \leq c_1, c_2 \leq 2$), r_1 and r_2 are random values ($0 \leq r_1, r_2 \leq 1$) regenerated for every velocity update, $v_k^{(s)}$ is the particle's velocity at iteration s, $x_k^{(s)}$ is the particle's position at iteration s, $\widehat{x}_k^{(s)}$ is the particle's individual best solution as of iteration s and $g^{(s)}$ is the swarm's best solution as of time iteration s.

If at the end of the method, for a certain particle there is a position $x_k^{(s)}$ that is not feasible for any of the decision variables, then the branch-and-bound technique is applied in an additional iteration.

2.3.2. Pareto frontier analysis

As a result of each optimization problem for each parameter ε_j, an optimum of the function f_j is obtained as a composition of the values of the functions f_{1_j} and f_{2_j} by virtue of equation [19]. The points (f_{1_j}, f_{2_j}) form the so-called Pareto frontier. It is necessary to consider all the possible solutions in this frontier and select some of them based on the appropriate value of ε_j and other conditions on the decision variables in the set of solutions.

All the exposed optimization methodology is summarized in the flowchart shown in Fig. 2, where $\Delta\varepsilon$ can be 0.1, for instance.

3. Case study description

The situation of the town selected for this case study, Aras de los Olmos, has a series of characteristics that are especially important to illustrate the method. Firstly, the town is located at the far end of a long 20 kV line, which causes many power supply problems and poor reliability. Secondly, in the town there are flat and elevated areas where

Table 1
Particle swarm optimization algorithm options.

Option	Description	Value
SwarmSize	Number of particles	50
FunctionTolerance	The algorithm stops if after 20 stall iterations a relative change in best fitness is less than this amount	10^{-6}
MaxIterations	Maximum number of iterations	1000
InertiaRange	Lower and upper bound of the adaptive inertia	0.1–0.9
SelfAdjustmentWeight	Weighting of each particle's best position when adjusting velocity, c_1	2
SocialAdjustmentWeight	Weighting of the neighbourhood's best position when adjusting velocity, c_2	2
MinNeighborsFraction	Minimum adaptive neighbourhood size (%)	25 %
nvars	Number of decision variables in this study: P_{PV}, P_P, P_T, P_{BM}, P_W in kW. They correspond to the installed power of PV, pumps, turbines, biomass and wind.	5
VariableBounds	Minimum and Maximum values for each decision variable (kW)	$P_{PV} : 0 \div 1000$ $P_P : 0 \div 250$ $P_T : 0 \div 250$ $P_{BM} : 0 \div 250$ $P_W : 0 \div 200$
StorageLimit	Maximum value of energy stored in the hydroelectric power plant (kWh)	$E_{H_{max}} = 7500$

Table 2
Costs considered for each resource.

Resource	Installation costs (€/kW)	Operation and maintenance costs (€/kW/year)	Production costs (€/kWh)
PV	1500	18	–
Pumps	3500	34	–
Turbines	3500	34	–
Biomass	7550	63	0.06
Wind	4200	44	–

wind and PV plants can be located. Thirdly, there are a large number of farms from which a large amount of biomass can be obtained at a low cost for a biogas plant. Finally, there is a river next to which there is a steep area with a drop of more than 100 m, ideal for installing a hydroelectric plant.

In this municipality, the demand and available resources have been studied, locating the plants in the best places, taking into account aspects such as performance, cost and regulation. All permits have been requested to install a biogas plant (up to 250 kW), PV plant (up to 1 MW), wind power plant (due to regulation, it is limited to 200 kW) and hydraulic plant (pumps and turbines up to 250 kW, trying to install more power from pumps than from turbines).

4. Results and discussion

The proposed methodology has been applied to the case study described in Section 3. The method has been programmed in MATLAB and the PSO algorithm configuration is shown in Table 1. A thorough parameter sweep analysis has been conducted to identify configurations with optimal performance characteristics for this study.

In each iteration of every particle, the program solves the simulated demand and generation of all resources based on the measured curves and analysis data of each resource for a full year. This simulation is extrapolated to a horizon (project lifetime) of 20 years.

To obtain the annualized costs, an interest rate of 0.6 % has been considered. Regarding the costs considered for each resource, manufacturers and maintenance companies have been consulted and the values in Table 2 have been proposed.
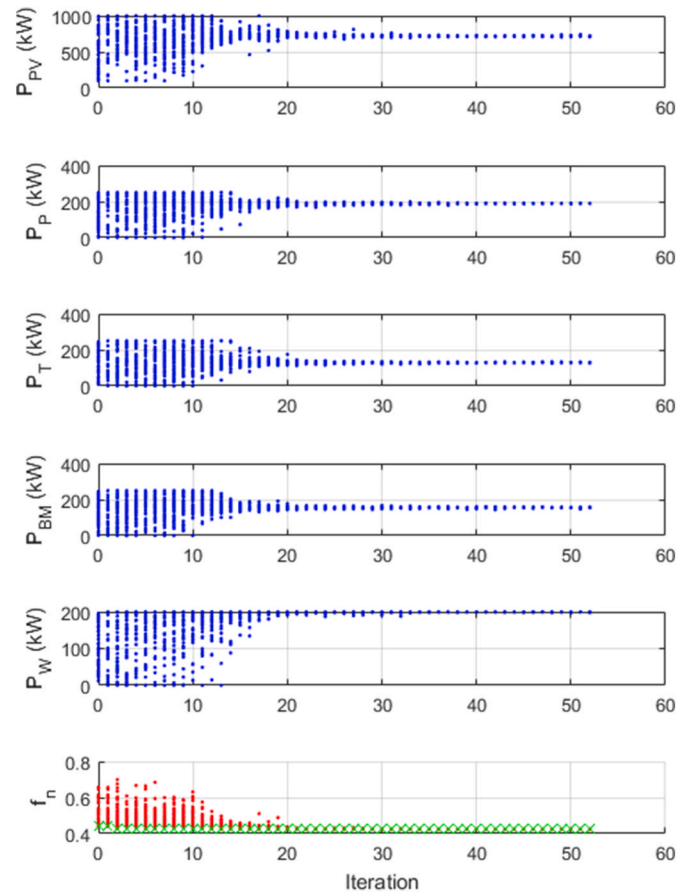

Fig. 3. Evolution of the particle swarm optimization algorithm for the case $\varepsilon_8 = 0.7$.

The expenses detailed in Table 2 encompass several key components. These comprise the labour costs essential for the operation of installations such as biomass and hydroelectric facilities, as well as the expenditures associated with the collection and transportation of biomass, and all financial outlays related to hydraulic tanks. Furthermore, the expenses linked to the acquisition of essential land and permits have been factored into the cost calculations. Concerning the pricing of energy imported from the network, it exhibits a variable nature, predicated on actual data obtained from a specific year, for which detailed information pertaining to the hourly demand curve is accessible [54]. The mean cost stands at 0.15€/kWh, and an annual increment of 0.5 % has been considered. These cost assessments have been derived subsequent to the development of a series of preliminary projects focused on renewable installations within the municipality under study. It is noteworthy that for prospective research endeavours, additional resources and databases, such as [55], are available for reference.

In the hydroelectric plant, an efficiency of 80 % has been considered for both pumps and turbines [56]. These values apply to incoming and outgoing energy, including load losses or alternator efficiency.

When normalizing the objective function, the values $f_{1_{max}} = 600,000€/year$ and $f_{2_{max}} = 4,000,000 kWh/year$ have been considered to keep both functions below 1 in any normal scenario.

The algorithm has been used to solve the 11 optimization problems that result from applying the coefficients shown in equation [24]. The number of simulated scenarios in this case study is deemed sufficient; however, in cases where the Pareto front is not distinctly delineated, it may be necessary to compute a higher number of scenarios, thereby reducing the discretization steps.
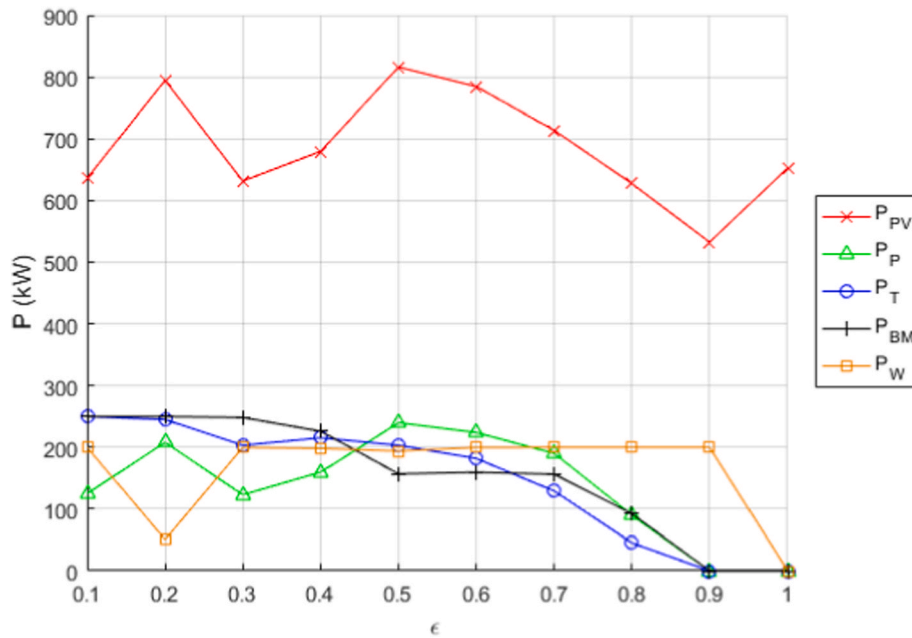
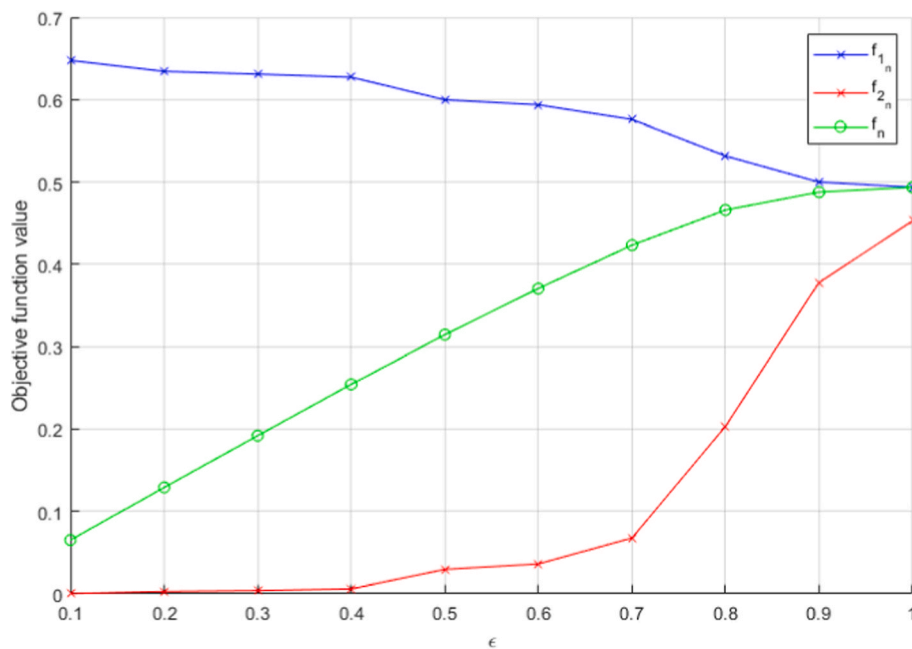**Fig. 4.** Final solution of the optimal mix reached for each ε.

Fig. 5. Value of functions f, f₁ and f₂ after solving each ε.

$$\varepsilon_j = \frac{j-1}{10}, \forall j \epsilon [1,11] \qquad (22)$$

In each problem, the 50 particles start out randomly covering the entire space and try to minimize the function f. As an example of the evolution of the PSO algorithm, the case $\varepsilon_8 = 0.7$ is shown in Fig. 3.

In Fig. 3, five graphs are shown with the positions of all the particles throughout the 52 iterations. The lower plot shows the value of the objective function for each particle in red and the best fitness of each iteration is highlighted in green. The iterations are represented on the horizontal axis. As can be seen, fitness tends to a minimum value and each variable tends to a value.

The final solution of the optimal mix reached for each problem is shown in Fig. 4.

The solution to the problem corresponding to $\varepsilon_1 = 0$ has been discarded, since $f = f_2$ for that case. This produces undesirable results, since the f_2 function is nullified in all scenarios where the decision variables take on large values. Therefore, the method cannot converge to an optimal solution. The value of functions f, f_1 and f_2 after solving each problem can be seen in Fig. 5. As is logical, when f_2 increases, f_1 decreases, since the objective is to minimize the value of f and at higher installed powers, less energy imported from the network.

As a result of all the iterations of all the problems, the different solutions of the objective function f and of each of its components f_1 and f_2. are obtained. A solution is called non-dominated or Pareto optimal, if none of the objective functions can be improved in value without degrading some of the other objective values. The set of non-dominated
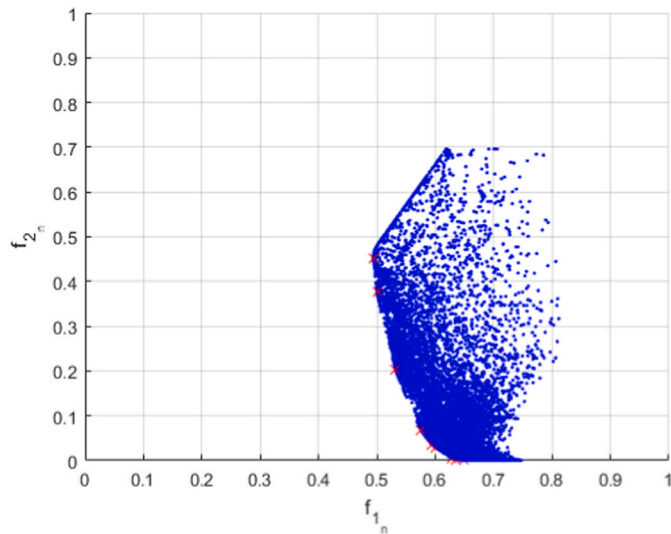
Fig. 6. Pareto frontier. All particles in each iteration (blue) and final convergence (red). (For interpretation of the references to colour in this figure legend, the reader is referred to the Web version of this article.)

solutions forms the so-called Pareto frontier for this problem. Fig. 6 shows the values of both objective functions for all the particles, highlighting in red the non-dominated solutions, belonging to the frontier.

Table 3 shows the combination of input variables that is considered optimal for each problem and the results of the objective functions.

The results from the Pareto frontier represent optimal outcomes based on the initial premises. Upon closer examination of each case, a specific set of decision variable values must be discussed to yield the feasible optimum through the Branch and Bound (BAB) method. This discussion underscores the importance of not only identifying Pareto-optimal solutions but also understanding the practical implications of these solutions in terms of real-world implementation. Through this thorough analysis, the study aims to provide a comprehensive view of the potential energy mix configurations that align with the project's objectives and constraints. Additionally, it is crucial to note that when selecting the optimal combination along the Pareto frontier, there are additional constraints to consider, particularly system stability. Therefore, each case must be analyzed with particular care. In the context of this case study, the sources contributing to system inertia are biogas, hydroelectric, and wind power. Hence, maintaining a minimum power of 50 kW from these sources is of great interest to ensure proper frequency control. This requirement highlights the importance of a meticulous examination of the energy mix to guarantee both economic efficiency and system reliability.

In a first consideration, both objective functions are important. To choose the optimal solution, a value of $\varepsilon_j \in [0.2, 0.8]$ should be selected, while extreme solutions should be avoided. Specifically, the solution for $\varepsilon_1 = 0$ does not make sense and has already been discarded from this

Table 4
Percentage increase of each objective function when the value of ε_j is increased.

ε_j	f_1	Δf_1	f_2	Δf_2
0.2	0.6342	−2.06 %	0.0028	704.19 %
0.3	0.6309	−0.53 %	0.0039	38.11 %
0.4	0.6272	−0.59 %	0.0059	52.63 %
0.5	0.5997	−4.38 %	0.0295	396.05 %
0.6	0.5937	−1.01 %	0.0360	22.24 %
0.7	0.5758	−3.00 %	0.0676	87.83 %
0.8	0.5318	−7.66 %	0.2033	200.49 %

Table 5
Viable powers of each source.

Resource	Feasible powers (kW)
P_{PV}	700-750-800
P_P	180-200-240
P_T	120-160-180-200
P_{BM}	120-160-200
P_W	100–200

Table 6
Optimal feasible solutions.

ε_j	P_{PV}	P_P	P_T	P_{BM}	P_W	f_1	f_2	f_n
0.6	750	240	180	160	200	0.5883	0.0393	0.4236
0.7	750	180	160	160	200	0.5800	0.0619	0.4246

table, since the algorithm cannot converge to a single optimum if only minimizing the function f_2 is considered as the objective.

Table 4 shows the percentage increase of each objective function when the value of ε_j is increased. Analyzing the evolution of the function f_1 and especially f_2, it is observed that the increase that occurs when going from $\varepsilon_8 = 0.7$ to $\varepsilon_9 = 0.8$ is very high. In the case of the function f_1, there is a reduction of 7.66 %, the largest of all. On the other hand, the function f_2 presents an increase of 200.49 %, much greater than the immediately previous values. Analogous instances arise when the solution is characterized by $\varepsilon_6 = 0.5$, suggesting that such solutions should be avoided, as this analysis pertains to a minimization problem. This is the first indication that the optimal solution to adopt may be the one corresponding to $\varepsilon_8 = 0.7$ or close to it.

Another argument for opting for this solution is that the mix is logical. This is so because it presents balanced values for pumps and turbines (somewhat higher for the pumps, as would be expected in a real mini-hydroelectric plant), a significant but reasonable percentage of PV and a balanced share of all resources.

Another equally acceptable solution would be the one corresponding to $\varepsilon_7 = 0.6$, but logically, this has a higher annualized cost, which is not very attractive for investors, so that when faced with two consecutive optimal solutions, the second can be considered more attractive. Both options are very similar, since it is a similar mix with little difference in the power of the different resources.

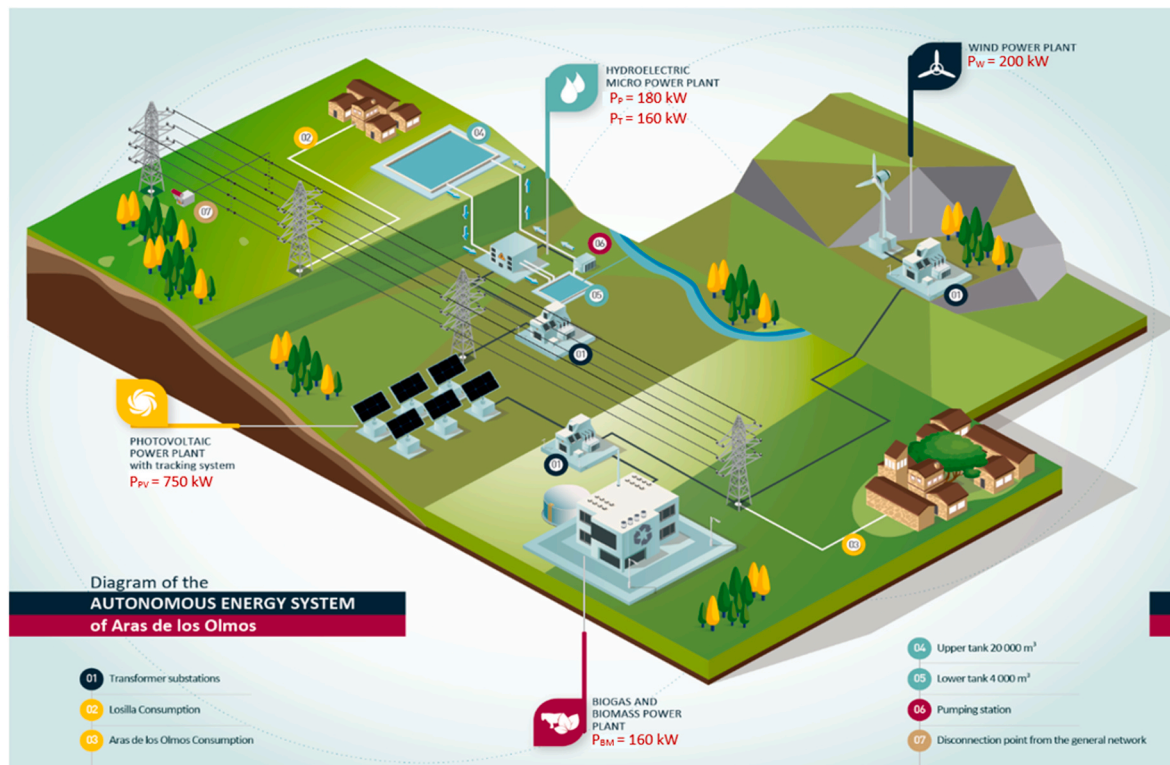To complete the proposed methodology, the BAB methodology must

Table 3
Results of the objective functions for each ε.

ε_j	P_{PV}	P_P	P_T	P_{BM}	P_W	f_1	f_2	f_n
0.1	636.08	124.74	250.00	250.00	200.00	0.6476	0.0004	0.0651
0.2	794.33	208.12	245.10	249.93	50.56	0.6342	0.0028	0.1291
0.3	631.49	122.96	203.20	248.45	199.82	0.6309	0.0039	0.1920
0.4	679.56	159.70	215.46	226.12	198.22	0.6272	0.0059	0.2544
0.5	815.86	239.93	203.35	156.95	193.95	0.5997	0.0295	0.3146
0.6	784.49	224.04	182.08	159.60	199.76	0.5937	0.0360	0.3706
0.7	713.60	190.21	129.19	156.45	200.00	0.5758	0.0676	0.4234
0.8	627.38	90.00	45.28	92.35	200.00	0.5318	0.2033	0.4661
0.9	532.22	0.00	0.00	0.00	200.00	0.5001	0.3780	0.4879
1.0	652.89	0.00	0.00	0.00	0.00	0.4937	0.4529	0.4937

Fig. 7. Autonomous energy system of Aras de los Olmos.

be applied to select the best feasible solution. In the range of preselected solutions, the viable powers of each source shown in Table 5 are considered, corresponding to real commercial equipment considered for the initial feasibility study. In this context, it is essential to note that considering system stability is crucial when evaluating the selected solutions. In the case study, photovoltaic generation does not contribute to system inertia, which makes solutions with small values in the other sources (e.g., less than 50 kW for any of them) potentially challenging for system stability. Therefore, it becomes of utmost importance to account for the Lowest Permissible Sustained Power, a factor that was initially left unrestricted in this study but is revisited after convergence in the discussion of optimal choices. This reconsideration is pivotal for initiating the Branch and Bound (BAB) process and ultimately selecting the definitive energy matrix.

All combinations have been simulated for both selected scenarios. The results of these simulations have produced the two optimal feasible solutions shown in Table 6.

Finally, it has been decided to opt for the solution corresponding to $\varepsilon_8 = 0.7$, particularized for the discrete values of the variables shown in Table 6, due to the similarity between both and to having a lower value in the annualized costs. In this case, the outcome with $\varepsilon_7 = 0.6$, while closely resembling that with $\varepsilon_8 = 0.7$, exhibits a slight imbalance. Notably, there is a significant disparity between the power generated by turbines and that by pumps, with the latter being approximately 33 % higher. Taking into consideration these factors, the practical design phase ultimately favoured the implementation of the solution corresponding to $\varepsilon_8 = 0.7$. As a result of the application of this method, theoretical configurations that minimize costs and imported grid energy have been obtained, providing tangible benefits for energy sustainability. After making the final decision of the desired scenario to be installed, the detailed design projects for the facilities have been developed, of which some particular aspects are described in the following section.

5. Technical implementation of the optimal solution

This section presents the specific physical design details of each system selected for the optimal solution of the renewable generation system in the proposed MG, aiming to demonstrate its feasibility. Fig. 7 illustrates the main characteristics of the renewable power plants.

5.1. Photovoltaic power plant

The construction features of the 750 kW PV power plant include 2400 polycrystalline PV solar panels, with each panel having a power of 315 kWp. The dimensions of each panel are 1956 x 992 × 40 mm. The panels are grouped in strings of 20 elements in series.

There are 6 inverters of 126 kWp (with a capacity to support up to 160 kWp and provide a 100 kW output) connected to the transformer. Each inverter is connected to a total of 20 strings (i.e., 400 panels). Since off-grid supply is planned, the inverters have an adjustable power factor and can supply up to 60 kvar.

The structure allows for the panels to be positioned at an angle of 35° or with solar tracking on one axis. The total surface area required in both cases is 10,000 m².

Finally, the energy will be evacuated in high voltage (HV) via a newly constructed power line from the transformer room to the connection with the existing 20 kV line.

5.2. hydroelectric power plant

The hydroelectric power plant will serve both as an energy storage and generation element. It has a turbinating capacity of 160 kW and a pumping capacity of 180 kW. The main elements are detailed below:

- An upper tank of asphalt concrete, raft type, with a surface area of 8100 m2 (90 x 90 × 3 m) to store 24,300 m³ of water, allowing for 48 turbinating hours.
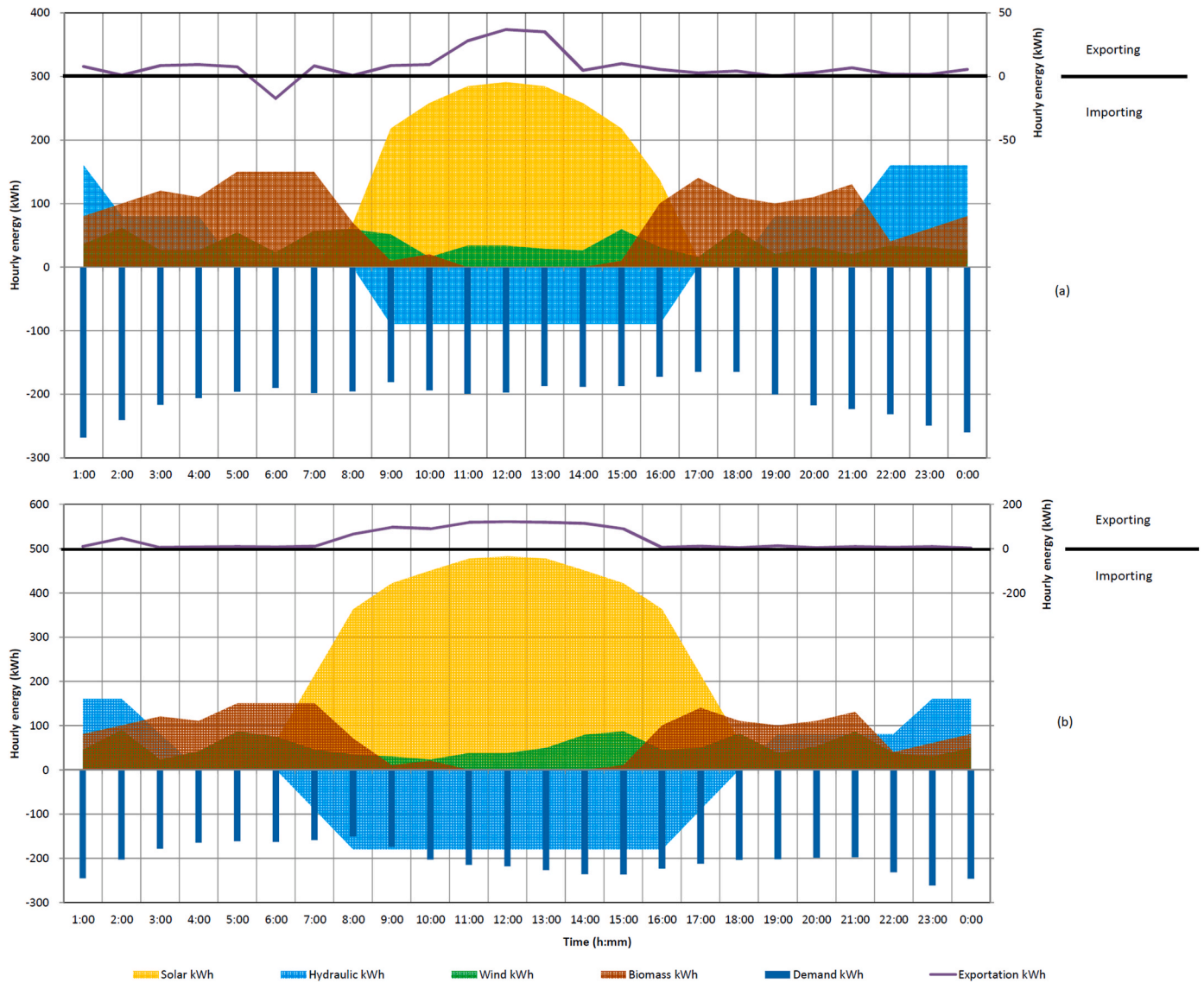
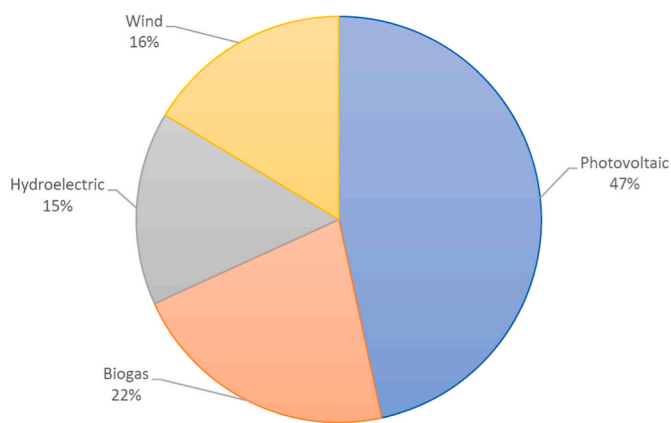Fig. 8. Management of all the resources. a) Winter day; b) Summer day.

Fig. 9. Annual energy supply Breakdown by resource.

- The lower tank is made of reinforced concrete with dimensions of 50 x 20 × 4 m, to store 4000 m^3 of water and allowing for 9.6 turbi-nating hours.

- Two Pelton type turbines with 80 kW hydraulic power, operating at a height of 180 m and a flow rate of 58 l/s.
- Two synchronous generators capable of operating both in parallel with the grid and in island mode, allowing control of delivered reactive power, voltage regulation, and synchronization.
- Three 60 kW vertical centrifugal pumps, operating at a height of 186 m and a flow rate of 100 m^3/h. The estimated pumping capacity is 13 h due to the size of the lower reservoir.

The electrical power will be evacuated in HV from the 250 kVA transformer station.

5.3. Biomass power plant

The construction features of the 160 kW biomass power plant are specified as follows:

- A storage area with a volume of 93 m^3, equivalent to a three-day storage capacity. It will be a reinforced concrete construction with a diameter of 6.3 m and a depth of 3 m.
- The digester is designed with a volume of 925.15 m^3 and a daily biogas production of 977 m^3. It is made of reinforced concrete, with

Table 7

Economic viability of the optimal solution.

Costs		Incomes		Economic parameters	
Facilities	4,589,000 €	Sale of energy to household users	247,500 €/year	IRR for 20 years	8.33%
Purchase of energy in the first three years (during the execution of the installations)	82,500 €/year	Sale of surpluses to the system (average value during the useful life)	43,400 €/year	Accumulated cash balance for 20 years	1,686,738 €

dimensions of 13 m in diameter and 7 m in height. The digester is covered by a double-layer elastic membrane with a capacity of 500 m^3, allowing the biogas to be stored for at least 12 h. It is worth mentioning that this digester will utilize strategically bioaugmented microbial strains resulting from the EU-funded project: Natural and Synthetic Microbial Communities for Sustainable Production of Optimized Biogas (Ref.: 101000470) [57].

- The biogas generated is treated in a desulphurizer and subsequently processed in a dryer, which has a maximum processing flow rate of 80 m^3/h for energy generation in the combustion engine. The 160 kW internal combustion engine will drive the synchronous generator with one pair of poles at 3000 rpm for the generation of electrical energy, which will be evacuated in low voltage (LV) to the transformer room.

5.4. Wind power plant

The wind power plant consists of a single 200 kW wind turbine, model Garbi 200/28 of Electriwind, with a tower height of 40 m and a rotor diameter of 28 m. It is a three-bladed, synchronous generator machine with a gearbox, pitch angle control system, and variable speed operation. The installation occupies an area of 6900 m^2, considering the foundations (100 m^2) and the roads (6800 m^2).

The energy will be evacuated in HV from the transformer located next to the wind turbine, through a newly constructed 1700 m underground line connecting the wind turbine to the existing 20 kV line.

5.5. Technical viability

Based on the analysis of hourly demand curves for a full year and the statistical values of generation for each resource, the real operation of the system at each moment has been simulated to minimize the objective functions. Fig. 8 illustrates both a typical summer day (a) and a winter day (b), where the management of all the resources can be observed, taking advantage of solar surpluses for pumping, the use of biogas during hours with lower solar PV production, and maintaining very low import and export values.

As a final contribution, Fig. 9 presents the fraction of energy demanded by the municipality that would be supplied by each energy resource over the course of a typical year.

5.6. Economic viability

With the pre-design of the power plants described above, a simulation of a 20-year scenario of facility usage has been developed. This scenario considers the described plant sizes and includes all associated costs, such as project and installation costs, maintenance, raw materials, personnel, bank loans, fees, and taxes. The study also considers a loss of efficiency of 0.5 % due to aging and a stable energy demand, considering it is a rural area. The income from the sale of energy is considered for each year, with conservative prices of €50/MWh for exchanges with the bulk system (import or export) and €0.15/kWh for the sale of energy to the town's household users. Additionally, financing in the form of a non-refundable grant covering 50 % of the total installation cost has been considered. The results of this scenario are shown in Table 7.

6. Conclusions

This study introduces an innovative method for optimizing microgrid (MG) generation system sizing, particularly in scenarios characterized by unreliable connections to the electrical grid. The proposed approach involves a comprehensive analysis, encompassing demand assessments, evaluation of generation potential, resource selection, and strategic placement. A multi-objective particle swarm optimization (MOPSO) algorithm is employed, with a focus on minimizing both annualized costs and imported energy from the grid.

The key significance of this work lies in its innovative approach. The practical application of the proposed method to a real-world microgrid in a Spanish town has yielded valuable insights and outcomes. Notably, the study has successfully identified an optimal generation mix for the microgrid, a crucial step towards enhancing energy self-sufficiency. The selection of this feasible solution has been thoughtfully considered, taking into account key criteria and inherent limitations. Moreover, the approach achieves a harmonious representation of available resources.

This case study stands as a pioneering exemplar within Spain and holds the potential to establish the town as the country's first to disconnect from the national grid. As these installations near completion and transition into operational status, further investigations into disconnection prerequisites, such as battery storage and system inertia, will be essential. The utilization of actual production data from the facility will play a pivotal role in these assessments.

Moreover, it's particularly interesting to note that the presented method holds broader applicability. While its successful implementation in other locations hinges on the meticulous analysis of energy demand and renewable generation potential in the initial steps, this approach offers a versatile framework. Additionally, the flexibility of exploring alternative optimization algorithms beyond MOPSO further underscores its adaptability, as each algorithm brings its unique advantages to the table. This versatility opens up opportunities for a wide range of applications and underscores the enduring value of this research.

Credit author statement

Carlos Roldán-Blay: Conceptualization, Methodology, Software, Writing – original draft Reviewing and Editing, Project administration, Funding acquisition. Guillermo Escrivá-Escrivá.: Data curation, Writing-Reviewing and Editing. Carlos Roldán-Porta: Visualization, Investigation, Supervision. Daniel Dasí-Crespo: Writing- Reviewing and Editing, Investigation, Resources.

Declaration of competing interest

Data availability

The authors do not have permission to share data.

Acknowledgement

References

[1] Cheng L, Yu T. Game-theoretic approaches applied to transactions in the open and ever-growing electricity markets from the perspective of power demand response: an overview. IEEE Access 2019;7:25727–62. https://doi.org/10.1109/ACCESS.2019.2900356.

[2] Dasí-Crespo D, Roldán-Blay C, Escrivá-Escrivá G, Roldán-Porta C. Evaluation of the Spanish regulation on self-consumption photovoltaic installations. A case study based on a rural municipality in Spain. Renew Energy 2023. https://doi.org/10.1016/j.renene.2023.01.055.

[3] Szinai JK, Sheppard CJ, Abhyankar N, Gopal AR. Reduced grid operating costs and renewable energy curtailment with electric vehicle charge management. Energy Pol 2020;136:111051. https://doi.org/10.1016/j.enpol.2019.111051.

[4] Tang H, Wang S, Li H. Flexibility categorization, sources, capabilities and technologies for energy-flexible and grid-responsive buildings: state-of-the-art and future perspective. Energy 2021;219:119598. https://doi.org/10.1016/j.energy.2020.119598.

[5] Auguadra M, Ribó-Pérez D, Gómez-Navarro T. Planning the deployment of energy storage systems to integrate high shares of renewables: the Spain case study. Energy 2023;264:126275. https://doi.org/10.1016/j.energy.2022.126275.

[6] Gunkel PA, Bergaentzlé C, Jensen IG, Scheller F. From passive to active: flexibility from electric vehicles in the context of transmission system development. Appl Energy 2020;277:115526. https://doi.org/10.1016/j.apenergy.2020.115526.

[7] Xie R, Wei W, Li M, Dong Z, Mei S. Sizing capacities of renewable generation, transmission, and energy storage for low-carbon power systems: a distributionally robust optimization approach. Energy 2023;263:125653. https://doi.org/10.1016/j.energy.2022.125653.

[8] Gielen D, Boshell F, Saygin D, Bazilian MD, Wagner N, Gorini R. The role of renewable energy in the global energy transformation. Energy Strategy Rev 2019; 24:38–50. https://doi.org/10.1016/j.esr.2019.01.006.

[9] Garg VK, Sharma S. Overview on microgrid system. In: 2018 Fifth international conference on parallel, distributed and grid computing (PDGC). IEEE; 2018, December. p. 694–9. https://doi.org/10.1109/PDGC.2018.8745849.

[10] Tomin N, Shakirov V, Kozlov A, Sidorov D, Kurbatsky V, Rehtanz C, Lora EE. Design and optimal energy management of community microgrids with flexible renewable energy sources. Renew Energy 2022;183:903–21. https://doi.org/10.1016/j.renene.2021.11.024.

[11] Delboni LF, Marujo D, Balestrassi PP, Oliveira DQ. Electrical power systems: evolution from traditional configuration to distributed generation and microgrids. Microgrids Design And Implementation 2019:1–25. https://doi.org/10.1007/978-3-319-98687-6_1.

[12] Altin N, Eyimaya SE. A review of microgrid control strategies. In: 2021 10th international conference on renewable energy research and application (ICRERA). IEEE; 2021, September. p. 412–7. https://doi.org/10.1109/ICRERA52334.2021.9598699.

[13] Garip S, Bilgen M, Altin N, Ozdemir S, Sefa İ. Reliability analysis of centralized and decentralized controls of microgrid. In: 2022 11th international conference on renewable energy research and application (ICRERA). IEEE; 2022, September. p. 557–61. https://doi.org/10.1109/ICRERA55966.2022.9922738.

[14] Song X, Zhang H, Fan L, Zhang Z, Peña-Mora F. Planning shared energy storage systems for the spatio-temporal coordination of multi-site renewable energy sources on the power generation side. Energy 2023;128976. https://doi.org/10.1016/j.energy.2023.128976.

[15] Djilali L, Vega CJ, Sanchez EN, Ruz-Hernandez JA. Distributed cooperative neural inverse optimal control of microgrids for island and grid-connected operations. IEEE Trans Smart Grid 2021;13(2):928–40. https://doi.org/10.1109/TSG.2021.3132640.

[16] Garces A. Small-signal stability in island residential microgrids considering droop controls and multiple scenarios of generation. Elec Power Syst Res 2020;185: 106371. https://doi.org/10.1016/j.epsr.2020.106371.

[17] Shahbazbegian V, Dehghani F, Shafiyi MA, Shafie-khah M, Laaksonen H, Ameli H. Techno-economic assessment of energy storage systems in multi-energy microgrids utilizing decomposition methodology. Energy 2023;283:128430. https://doi.org/10.1016/j.energy.2023.128430.

[18] Kharrich M, Mohammed OH, Kamel S, Aljohani M, Akherraz M, Mosaad MI. Optimal design of microgrid using chimp optimization algorithm. In: 2021 IEEE international conference on automation/XXIV congress of the Chilean Association of Automatic Control (ICA-ACCA. IEEE; 2021, March. p. 1–5. https://doi.org/10.1109/ICAACCA51523.2021.9465336.

[19] Ribó-Pérez D, Bastida-Molina P, Gómez-Navarro T, Hurtado-Pérez E. Hybrid assessment for a hybrid microgrid: a novel methodology to critically analyse generation technologies for hybrid microgrids. Renew Energy 2020;157:874–87. https://doi.org/10.1016/j.renene.2020.05.095.

[20] Wu K, Li Q, Chen Z, Lin J, Yi Y, Chen M. Distributed optimization method with weighted gradients for economic dispatch problem of multi-microgrid systems. Energy 2021;222:119898. https://doi.org/10.1016/j.energy.2021.119898.

[21] Haidar AM, Fakhar A, Helwig A. Sustainable energy planning for cost minimization of autonomous hybrid microgrid using combined multi-objective optimization

[22] Kanakadhurga D, Prabaharan N. Demand side management in microgrid: a critical review of key issues and recent trends. Renew Sustain Energy Rev 2022;156: 111915. https://doi.org/10.1016/j.rser.2021.111915.

[23] Fioriti D, Lutzemberger G, Poli D, Duenas-Martinez P, Micangeli A. Coupling economic multi-objective optimization and multiple design options: a business-oriented approach to size an off-grid hybrid microgrid. Int J Electr Power Energy Syst 2021;127:106686. https://doi.org/10.1016/j.ijepes.2020.106686.

[24] Bie Z, Lin Y, Li G, Li F. Battling the extreme: a study on the power system resilience. Proc IEEE 2017;105(7):1253–66. https://doi.org/10.1109/JPROC.2017.2679040.

[25] Kroposki B. Integrating high levels of variable renewable energy into electric power systems. J Modern Power Syst Clean Energy 2017;5(6):831–7. https://doi.org/10.1007/s40565-017-0339-3.

[26] Daneshvar M, Mohammadi-Ivatloo B, Abapour M, Asadi S. Energy exchange control in multiple microgrids with transactive energy management. J Modern Power Syst Clean Energy 2020;8(4):719–26. https://doi.org/10.35833/MPCE.2018.000590.

[27] Armendariz M, Heleno M, Cardoso G, Mashayekh S, Stadler M, Nordström L. Coordinated microgrid investment and planning process considering the system operator. Appl Energy 2017;200:132–40. https://doi.org/10.1016/j.apenergy.2017.05.076.

[28] Norouzi F, Hoppe T, Elizondo LR, Bauer P. A review of socio-technical barriers to Smart Microgrid development. Renew Sustain Energy Rev 2022;167:112674. https://doi.org/10.1016/j.rser.2022.112674.

[29] Ghandehariun S, Ghandehariun AM, Ziabari NB. Performance prediction and optimization of a hybrid renewable-energy-based multigeneration system using machine learning. Energy 2023:128908. https://doi.org/10.1016/j.energy.2023.128908.

[30] Naz MN, Mushtaq MI, Naeem M, Iqbal M, Altaf MW, Haneef M. Multicriteria decision making for resource management in renewable energy assisted microgrids. Renew Sustain Energy Rev 2017;71:323–41. https://doi.org/10.1016/j.rser.2016.12.059.

[31] Vilaisarn Y, Rodrigues YR, Abdelaziz MMA, Cros J. A deep learning based multiobjective optimization for the planning of resilience oriented microgrids in active distribution system. IEEE Access 2022;10:84330–64. https://doi.org/10.1109/ACCESS.2022.3197194.

[32] Irshad AS, Samadi WK, Fazli AM, Noori AG, Amin AS, Zakir MN, Senjyu T. Resilience and reliable integration of PV-wind and hydropower based 100% hybrid renewable energy system without any energy storage system for inaccessible area electrification. Energy 2023:128823. https://doi.org/10.1016/j.energy.2023.128823.

[33] Wang Y, Cui Y, Li Y, Xu Y. Collaborative optimization of multi-microgrids system with shared energy storage based on multi-agent stochastic game and reinforcement learning. Energy 2023:128182. https://doi.org/10.1016/j.energy.2023.128182.

[34] Liu J, Ma L, Wang Q. Energy management method of integrated energy system based on collaborative optimization of distributed flexible resources. Energy 2023; 264:125981. https://doi.org/10.1016/j.energy.2022.125981.

[35] Obara SY, Sato K, Utsugi Y. Study on the operation optimization of an isolated island microgrid with renewable energy layout planning. Energy 2018;161: 1211–25. https://doi.org/10.1016/j.energy.2018.07.109.

[36] Sousa J, Lagarto J, Camus C, Viveiros C, Barata F, Silva P, Paraíba O. Renewable energy communities optimal design supported by an optimization model for investment in PV/wind capacity and renewable electricity sharing. Energy 2023; 283:128464. https://doi.org/10.1016/j.energy.2023.128464.

[37] Roldán-Blay Carlos, et al. Optimal generation scheduling with dynamic profiles for the sustainable development of electricity grids. Sustainability 2019;11(24):7111. https://doi.org/10.3390/su11247111.

[38] Memon SA, Patel RN. An overview of optimization techniques used for sizing of hybrid renewable energy systems. Renewable Energy Focus 2021;39:1–26. https://doi.org/10.1016/j.ref.2021.07.007.

[39] Borhanazad H, Mekhilef S, Ganapathy VG, Modiri-Delshad M, Mirtaheri A. Optimization of micro-grid system using MOPSO. Renew Energy 2014;71:295–306. https://doi.org/10.1016/j.renene.2014.05.006.

[40] Li R, Guo S, Yang Y, Liu D. Optimal sizing of wind/concentrated solar plant/electric heater hybrid renewable energy system based on two-stage stochastic programming. Energy 2020;209:118472. https://doi.org/10.1016/j.energy.2020.118472.

[41] Chang J, Li Z, Huang Y, Yu X, Jiang R, Huang R, Yu X. Multi-objective optimization of a novel combined cooling, dehumidification and power system using improved M-PSO algorithm. Energy 2022;239:122487. https://doi.org/10.1016/j.energy.2021.122487.

[42] Ramírez-Ochoa DD, Pérez-Domínguez LA, Martínez-Gómez EA, Luviano-Cruz D. PSO, a swarm intelligence-based evolutionary algorithm as a decision-making strategy: a review. Symmetry 2022;14(3):455. https://doi.org/10.3390/sym14030455.

[43] Tomazella CP, Nagano MS. A comprehensive review of Branch-and-Bound algorithms: guidelines and directions for further research on the flowshop scheduling problem. Expert Syst Appl 2020;158:113556. https://doi.org/10.1016/j.eswa.2020.113556.

[44] Fan Y, Wang P, Heidari AA, Chen H, Mafarja M. Random reselection particle swarm optimization for optimal design of solar photovoltaic modules. Energy 2022;239:121865. https://doi.org/10.1016/j.energy.2021.121865.

[45] Selvakumar K, Anuradha R, Arunkumar AP. Techno-economic assessment of a hybrid microgrid using PSO. Mater Today Proc 2022;66:1131–9. https://doi.org/10.1016/j.matpr.2022.04.919.

[46] Copp DA, Nguyen TA, Byrne RH, Chalamala BR. Optimal sizing of distributed energy resources for planning 100% renewable electric power systems. Energy 2022;239:122436. https://doi.org/10.1016/j.energy.2021.122436.

[47] Chaduvula H, Das D. Analysis of microgrid configuration with optimal power injection from grid using point estimate method embedded fuzzy-particle swarm optimization. Energy 2023:128909. https://doi.org/10.1016/j.energy.2023.128909.

[48] Fioriti D, Poli D, Duenas-Martinez P, Micangeli A. Multiple design options for sizing off-grid microgrids: a novel single-objective approach to support multi-criteria decision making. Sustain Energy, Grids and Netw 2022;30:100644. https://doi.org/10.1016/j.segan.2022.100644.

[49] Raya-Armenta JM, Bazmohammadi N, Avina-Cervantes JG, Sáez D, Vasquez JC, Guerrero JM. Energy management system optimization in islanded microgrids: an overview and future trends. Renew Sustain Energy Rev 2021;149:111327. https://doi.org/10.1016/j.rser.2021.111327.

[50] Escrivá-Escrivá Guillermo, Roldán-Blay Carlos, Álvarez-Bel Carlos. Electrical consumption forecast using actual data of building end-use decomposition. Energy Build 2014;82:73–81. https://doi.org/10.1016/j.enbuild.2014.07.024.

[51] Roldán-Blay C, Escrivá-Escrivá G, Roldán-Porta C, Álvarez-Bel C. An optimisation algorithm for distributed energy resources management in micro-scale energy hubs. Energy 2017;132:126–35. https://doi.org/10.1016/j.energy.2017.05.038.

[52] Mohammed OH, Kharrich M. An overview of the performance of PSO algorithm in renewable energy systems. In: Applying Particle Swarm Optimization: New Solutions and Cases for Optimized Portfolios; 2021. p. 307–20. https://doi.org/10.1007/978-3-030-70281-6_16.

[53] Rui L, Wang X, Zhang Y, Wang X, Qiu X. A self-adaptive and fault-tolerant routing algorithm for wireless sensor networks in microgrids. Future Generat Comput Syst 2019;100:35–45. https://doi.org/10.1016/j.future.2019.04.024.

[54] Analysis, ESIOS electricity data transparency [WWW Document], n.d. URL, https://www.esios.ree.es/es (accessed on 2023, June 12).

[55] Open Energy Information—Transparent Cost Database. Available online: https://openei.org/apps/TCDB/(accessed on May 2023)].

[56] Singh VK, Singal SK. Operation of hydro power plants-a review. Renew Sustain Energy Rev 2017;69:610–9. https://doi.org/10.1016/j.rser.2016.11.169.

[57] Natural and Synthetic Microbial Communities for Sustainable Production of Optimised Biogas (Micro4Biogas – Horizon; 2020, 101000470. https://micro4biogas.eu/. [Accessed 12 June 2023].